Myb10-D confers *PHS-3D* resistance to pre-harvest sprouting by regulating *NCED* in ABA biosynthesis pathway of wheat

Jing Lang[1]*, Yuxin Fu[1,2]*, Yong Zhou[1]*, Mengping Cheng[1], Min Deng[1], Maolian Li[1], Tingting Zhu[3], Jian Yang[1], Xiaojiang Guo[1,4], Lixuan Gui[1], Linchuan Li[1], Zhongxu Chen[1], Yingjin Yi[1,3], Lianquan Zhang[1] (iD), Ming Hao[1] (iD), Lin Huang[1], Chao Tan[1], Guoyue Chen[1], Qiantao Jiang[1], Pengfei Qi[1] (iD), Zhien Pu[1], Jian Ma[1], Zehou Liu[1], Yujiao Liu[1], Ming-Cheng Luo[3] (iD), Yuming Wei[1,5], Youliang Zheng[1,5], Yongrui Wu[2] (iD), Dengcai Liu[1,5] (iD) and JiRui Wang[1,5] (iD)

[1]Triticeae Research Institute, Sichuan Agricultural University, Chengdu 611130, China; [2]CAS Center for Excellence in Molecular Plant Science, Chinese Academy of Sciences, Shanghai 210027, China; [3]Department of Plant Biology, University of California, Davis, CA 95616, USA; [4]Department of Plant Science, University of California, Davis, CA 95616, USA; [5]State Key Laboratory of Crop Gene Exploration and Utilization in Southwest China, Sichuan Agricultural University, Chengdu 611130, China

Summary

• Pre-harvest sprouting (PHS), the germination of grain before harvest, is a serious problem resulting in wheat yield and quality losses.

• Here, we mapped the PHS resistance gene *PHS-3D* from synthetic hexaploid wheat to a 2.4 Mb presence–absence variation (PAV) region and found that its resistance effect was attributed to the pleiotropic *Myb10-D* by integrated omics and functional analyses.

• Three haplotypes were detected in this PAV region among 262 worldwide wheat lines and 16 *Aegilops tauschii*, and the germination percentages of wheat lines containing *Myb10-D* was approximately 40% lower than that of the other lines. Transcriptome and metabolome profiling indicated that *Myb10-D* affected the transcription of genes in both the flavonoid and abscisic acid (ABA) biosynthesis pathways, which resulted in increases in flavonoids and ABA in transgenic wheat lines. *Myb10-D* activates 9-*cis*-epoxycarotenoid dioxygenase (*NCED*) by biding the secondary wall MYB-responsive element (SMRE) to promote ABA biosynthesis in early wheat seed development stages.

• We revealed that the newly discovered function of *Myb10-D* confers PHS resistance by enhancing ABA biosynthesis to delay germination in wheat. The PAV harboring *Myb10-D* associated with grain color and PHS will be useful for understanding and selecting white grained PHS resistant wheat cultivars.

Introduction

Common wheat (*Triticum aestivum*, AABBDD) is a staple food crop for more than one-third of the global human population and provides *c.* 20% of the calories consumed by humans globally (Shewry & Hey, 2015). The availability of reference sequences and the rise of the pangenome project of wheat have allowed the identification of genes and their structural variations that involve the single-nucleotide polymorphisms (SNPs) and the loss of genomic regions encoding protein-coding genes in some individuals (i.e. presence–absence variation, PAV) (Uauy, 2017; Jia *et al.*, 2018; Walkowiak *et al.*, 2020; Zhang *et al.*, 2021). The pangenome of a species is composed of the core genome that is present in all individuals and the dispensable genome (PAV) that is present in some individuals of a species (Morgante *et al.*, 2007; Marroni *et al.*, 2014). Polyploid genomes may also be more prone to containing structural variation that could play an important role in phenotypic variance (Schiessl *et al.*, 2018).

Wheat production in many countries, where rain tends to fall during the harvest season, is negatively impacted by pre-harvest sprouting (PHS), the precocious germination of grains before harvest. PHS is directly associated with reductions in both grain yield and flour quality. It is estimated that PHS damage is responsible for up to $1 billion in annual losses (Nakamura, 2018; Vetch *et al.*, 2019). In wheat, compared with red-grained cultivars, white-grained cultivars are characterized by more efficient flour extraction, a better ash content, a more favorable appearance and a less bitter taste in the final product (Ransom *et al.*, 2006). However, white-grained wheat has been reported to be more susceptible to PHS than red-grained wheat for more than 100 yr (Nilsson-Ehle, 1914; Gordon, 1979; Warner *et al.*, 2000). The pigment of red-grained wheat is presumed to be a result of the accumulation of the polyphenolic compound phlobaphene, which is derived from the precursor catechin and is

*These authors contributed equally to this work.

an end product of the flavonoid pathway (Miyamoto and Everson, 1958; Gordon, 1979). The R2R3-MYB transcription factor *Myb10*, located on wheat chromosomes 3A/3B/3D, encodes the *R-1* gene that controls redness by regulating the accumulation of anthocyanins (Groos *et al.*, 2002; Himi & Noda, 2005; Himi *et al.*, 2005; Himi *et al.*, 2011). *Myb10* is known to regulate flavones, flavonols, and proanthocyanidin by regulating many genes in the pathways of flavonoid biosynthesis (Lai *et al.*, 2013). PHS resistance genes that span the chromosomal region of Myb10 have been discovered in red-grained wheat (Groos *et al.*, 2002; Rasul *et al.*, 2009). However, the relationship between *Myb10* and PHS resistance genes is still unclear (Medina-Puche *et al.*, 2014).

Common wheat is an allopolyploid species originating from hybridization between tetraploid *Triticum turgidum* (AABB) (McFadden & Sears, 1946) and *Aegilops tauschii* (DD) (Kihara, 1944) in the Fertile Crescent, where little rain falls during the harvest season, and PHS is therefore rare (Nakamura, 2018). *Aegilops tauschii* exhibits a high degree of PHS resistance (Liu *et al.*, 1998). Hybrids have been recreated by crossing *T. turgidum* with *A. tauschii* to produce so-called synthetic hexaploid wheat (SHW) to analyze PHS resistance (Imtiaz *et al.*, 2008; Yang *et al.*, 2014). *PHS-3D* is an SHW-derived locus linked to *Myb10-D* (*TaMyb10* on D genome of wheat) and confers strong PHS resistance explaining up to 42.47% of PHS variation in seven environments (Yang *et al.*, 2019). Here, we demonstrate that *PHS-3D* is *Myb10-D* and negatively controls germination by activating 9-*cis*-epoxycarotenoid dioxygenase (*NCED*) transcription, which is involved in ABA biosynthesis; deepening grain color and increasing barriers to water uptake in wheat.

Materials and Methods

Plant materials

SHW-L1 is a medium PHS resistant synthetic wheat that carries *PHS-3D* (*QPhs.sicau-3D*) obtained from allohexaploidization between the deep seed dormancy *A. tauschii* AS60 (Liu *et al.*, 1998) and PHS-resistant *T. turgidum* AS2255 (Zhang *et al.*, 2004). Chuanmai32 (CM32) is a PHS susceptible cultivated wheat (Yu *et al.*, 2014). SHW-L1 and CM32 derived recombinant inbred lines (RILs) were evaluated for PHS resistance in nine independent environments (Yang *et al.*, 2019). One resistant RIL (RIL71) and one susceptible RIL (RIL143) were selected as parents to develop heterogeneous inbred family (HIF) populations with a total of 7500 $F_{3:4}$ HIF lines for fine mapping. We assayed $F_{2:3}$ lines with 17 pairs of KASP markers (Supporting Information Table S1) and generated enough $F_{3:4}$ seeds. Then $F_{3:4}$ lines with homozygous fragments were selected and phenotyped. The fine mapping population panel was planted in Chongzhou (30°36′27.02″N, 103°37′4.10″E) from 2016 to 2018 (2016-CZ, 2017-CZ, and 2018-CZ). Each line was single-seed planted in two 1.5 m long rows, with 50 cm between rows and 10 cm between plants within rows.

A natural population of 250 wheat from all over the world, as well as 16 accessions of diploid *A. tauschii* ($2n = 2x = 14$, DD),

and two accessions of tetraploid *T. turgidum* ssp. *durum* ($2n = 4x = 28$, AABB) were collected from the US Department of Agriculture (USDA) and Sichuan Agricultural University (SICAU) (Wang *et al.*, 2013; Zhou *et al.*, 2018), and their germination percentages (GPs) were assayed previously (Table S2) (Zhou *et al.*, 2017). These accessions were used to analyze the relationship between sequence variations and PHS resistance in wheat germplasms.

Evaluation of germination percentages and grain color

The wheat grain is a caryopsis with a pericarp. This article refers to the wheat caryopsis as a 'seed' for simplicity's sake. Both whole spikes and threshed seeds were used for the germination tests. The materials were harvested when the grains reached physiological maturity and then air-dried in the shade at room temperature until seed moisture was < 10%. Three replications of 50 threshed undamaged seeds were incubated in Petri dishes that contained filter paper in the lower half and 5 ml of distilled water at 20°C without light for 7 d. The GPs (i.e. total germinated seeds/total assayed seeds) was used to assay the germination level at 7 d after imbibition (DAI) (Walker-Simmons, 1988). For each independent plant, only mature grains from primary or secondary spikes were selected to be stored at −20°C until phenotyping. In total, 20 spikes collected from 16 plants were wrapped in moist filter paper after being immersed in distilled water for 6 h, and put in a dew chamber without light at 20°C for 7 d and photographs taken every day. Seeds in spikes were threshed and the GP was calculated on the seventh day (Paterson & Sorrells, 1990).

The seeds were scanned with an Uniscan M2800 Scanner (Unis, China) Series_V2.0, and the scanned images were analyzed by Photoshop CS6 straw tool (Stetter *et al.*, 2020). Seed colors were inferred visually from seed samples.

Evaluation of seed coat permeability

Seed coat permeability is important to study as it plays significant roles in seed dormancy and germination, thus the seed permeability was checked with the TTC (2,3,5-triphenyltetrazolium chloride) method (Roistacher *et al.*, 1957). During seed imbibition, higher permeability could be indicated by the deeper dyeing color of TTC. Germinating seeds of transgenic lines (overexpression, OE) and control (wild-type, WT) were added by 1% TTC and incubated at 37°C. The color variance of seeds was artificially assayed at 3, 6, 12, 24, 36, 48 and 60 h after imbibition (HAI), and used to determine seed coat permeability.

Genomic sequences data

The genomic reference data of Chinese Spring (ftp://ftp.ensemblgenomes.org/pub/plants/current/fasta/triticum_aestivum/dna/), AL8/78 (http://aegilops.wheat.ucdavis.edu/ATGSP/), Cadenza, and Robigous (https://opendata.earlham.ac.uk/opendata/data/Triticum_aestivum/EI/v1.1/) were obtained from the database. And the data of Aikang58 were obtained from Dr Jizeng Jia (Jia *et al.*, 2021) (Table S3). The genotyping data of 12 hexaploid

wheat and one tetraploid wheat cultivars from the wheat pan-genome database (http://www.10wheatgenomes.com/) were also analyzed (Walkowiak *et al.*, 2020).

Additional materials and methods

Details on the DNA extraction and genotyping (Methods S1), fine mapping of *PHS-3D* (*QPHS.sicau-3D*) (Methods S2), optical map construction (Methods S3), gene cloning and sequencing (Methods S4), RNA preparation and RNA sequencing (Methods S5), next-generation sequencing (NGS) data analysis (reads mapping, assembly, and functional annotation) (Methods S6), analysis of gene expression by quantitative polymerase chain reaction (qPCR) (Methods S7), gene transformation (Methods S8), endogenous ABA profiling (Methods S9), flavonoids extraction and profiling (multiple reaction monitoring, MRM) (Methods S10), subcellular localization of Myb10-D (Methods S11), RNA *in situ* hybridization (Methods S12), protein expression in *Escherichia coli* and purification (Methods S13), electrophoretic mobility shift assay (EMSA) (Methods S14), transient expression assay (Methods S15), yeast one-hybrid (Methods S16), statistical analyses (Methods S17), and code used in this study (Methods S18) can be found in the Supporting Information.

Results

PHS-3D is located within a large PAV region

PHS-3D (*QPHS.sicau-3D*) was previously detected in a RIL population between the synthetic wheat genotype SHW-L1 and common wheat cultivar Chuanmai 32 (CM32) (Yang *et al.*, 2014). Here, by mapping SNP markers in the region of *PHS-3D* (Fig. 1a), two RILs, i.e. the PHS resistant line L71 and susceptible line L143, were selected to develop HIF populations (Fig. 1b). A total of 7500 $F_{3:4}$ families that reckoned to the population comprising self-progenies of selected individuals with heterozygous *PHS-3D* from 50 $F_{2:3}$ plants. Then, we developed a total of 17 markers to fine-map *PHS-3D* using the Kompetitive Allele-Specific PCR (KASP) technique based on SNP in this region (Supporting Information Fig. S1; Table S1). By combining the genotype and phenotype, the *PHS-3D* region was narrowed to a 2.7 Mb region, flanking from K-AX-108730423 (572.2 Mb) to K-AX-111501911 (574.9 Mb). Though 12 out of 17 KASP markers were located in this 2.7 Mb region, their signal could not be detected in 836 PHSS $F_{3:4}$ lines. Thus, no further recombination was observed, which indicated that there was a lack of recombination (Fig. 1c).

The absence of recombination is related to a PAV. A total of 1534 Gb of large single molecules (> 150 Kb) labeled by the *DLE-1* enzyme was obtained from the PHS-susceptible cultivar CM32, and *de novo* assembled into a BioNano optical map. Taking advantage of the optical map, we identified a deletion (Chr3D: 571.5–574.4 Mb) in CM32 by aligning its genome sequence to the Chinese Spring (CS) genome sequences. Further sequence comparison revealed an ~2.4 Mb deletion in the common wheat cultivars Robigus, and Aikang58 (AK58, Chr3D:

583.6–583.7 Mb) (Fig. 1d) relative to CS (Chr3D: 571.9–574.3 Mb), Cadenza, and the synthetic wheat genotype SHW-L1 (Fig. 1e; Table S3). The deleted region resulted in the loss of 20 genes/pseudogenes (gene order: 16–35), whereas the genes flanking the PAV region (gene order: 1–15 and 36–49) were conserved (Table S4). The PAV region harbored 23 transposable elements (LTR/Copia, Gypsy, and TIR) in CS (Fig. 1f). Based on the molecular signatures at the breakpoints, unequal crossing over between TEs may have led to the PAV in wheat (Table S5).

The large PAV is associated with PHS resistance in wheat germplasms

We developed 14 sequence-tagged-site (STS) markers for genes/pseudogenes in the PAV region (Fig. S2; Tables S6) and carried out an association analysis using 16 *A. tauschii* (DD genome), three *T. turgidum* (AABB genome), and 262 hexaploid wheat (AABBDD genome) lines to assess the relationship between PAV and PHS resistance (Fig. 2a). As expected, no PCR products were detected in *T. turgidum* due to the absence of the D genome. A total of three haplotypes were identified among the wheat lines, i.e. Hap-I without a deletion, Hap-II with a 2.2 Mb deletion, and Hap-III with the whole 2.4 Mb deletion (Fig. 2b). Hap-I and Hap-III are more prevalent than Hap-II in common wheat. This 2.4 Mb region in common wheat is also conserved in 16 analyzed *A. tauschii* accessions collected from Caspian Sea areas.

The average GPs of the wheat lines of Hap-I (GP: 41.48%) were significantly lower than those of Hap-II (GP: 78.75%, $u = 8.55$) and Hap-III (GP: 81.69%, $u = 9.85$) (Fig. 2c; Table S2). In Hap-I, 98.44% of lines were predominately red (brown, tan)-grained, and only one landrace AS661609 (Tuotuomai), collected from China, was white-grained. The reduction in PHS resistance in Hap-II and Hap-III indicated that *PHS-3D* is probably located in the deleted region between *STS-Myb10* (572.2 Mb) and *STS-HRGP* (573.2 Mb).

Myb10-D is highly expressed in the seeds of PHS resistant wheat

The 20 genes located within the 2.4 Mb deleted region that probably harbors *PHS-3D* were used to identify the functional gene(s) that contribute to PHS resistance. Transcriptomic results obtained for seeds 12 and 24 HAI, seedling leaves, roots, and seeds 10, 20 and 30 d post-anthesis (DPA) were compared between SHW-L1 and CM32 (Fig. S3a; Table S6). All of the 20 analyzed genes were not expressed in CM32 at a level of transcripts per million (TPM) > 1, except *RS19* (gene #33, chloroplastic 30S ribosomal protein S19, which had 92 copies in the wheat genome). Three genes *Myb10*, *TAF9*, and *Oco1* were expressed in the seed of SHW-L1. *TAF9* is an orthologous gene for TATA-binding protein-associated factor 9 that is associated with salt and heat stress responses (Li *et al.*, 2017). *Oco1* is a homolog of oral cancer-overexpressed protein 1 (ORAOV1) (Jiang *et al.*, 2010). *Myb10-D* is known as an R2R3-MYB transcription factor. Then we checked their expression levels in 29 tissues/stages of CS and BCScv1 (Fig. S3b) (IWGSC *et al.*, 2018).
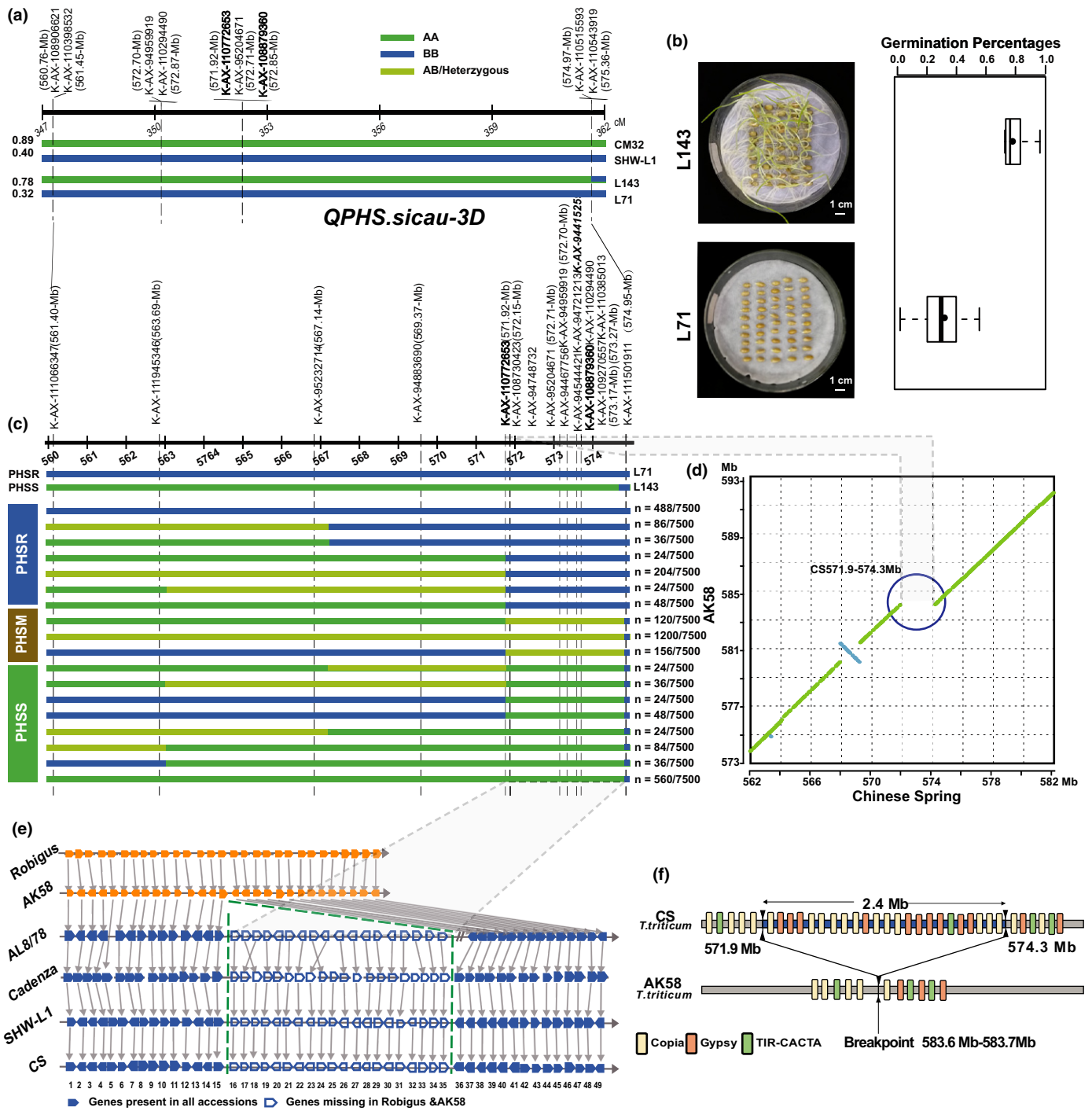
Fig. 1 Fine mapping and genomic analysis of *PHS-3D* from wheat (*Triticeae aestivum*). (a) QTL of the *QPHS.sicau-3D* (*PHS-3D*) region in pre-harvest sprouting (PHS)-resistant SHW-L1, PHS-susceptible CM32, and their recombinant inbred lines (RILs) L143 and L71. (b) The average germination percentage of L143 (77.1%) and L71 (29.6%) from six environments at 7 d after imbibition (DAI). (c) Fine mapping of *PHS-3D*. PHSR, PHSS, and PHSM indicated PHS resistance, susceptibility, and moderate resistance, respectively. The numbers on the right of the bar indicate the number of recombinants. The two markers (i.e. AX-108730423 and AX-108925806) were close to *PHS-3D*, and two markers (i.e. AX-110772653 and AX-108879360) were identified in our previous genome-wide association study (GWAS) and bi-parental QTL mapping analysis. The physical positions of 17 KASP markers are based on the IWGSC CS RefSeq v2.0 assembly. (d) The dot-plot shows a 2.4 Mb presence–absence variation (PAV) between Chinese Spring (CS) and Aikang58 (AK58). (e) Twenty annotated genes (gene order: 16-35) are missing in the PAV region. (f) Transposable elements, including LTR_copia, LTR_gypsy, and Tir_CACTA, are abundant in the PAV region. SD, error bars given in the graphs.

TAF9 and *OCO1* are highly expressed in all tissues (root, shoot, leaf, flower, and seed), with 18 and six orthologs in common wheat, respectively. *Myb10* is highly expressed in the seed (2DPA) and aleurone layer (12DPA). At last, we confirmed the high expression of *Myb10* in SHW-L1 at 5-15 DPA by qPCR (Fig. S3c). Thus, *Myb10-D* was prioritized for functional
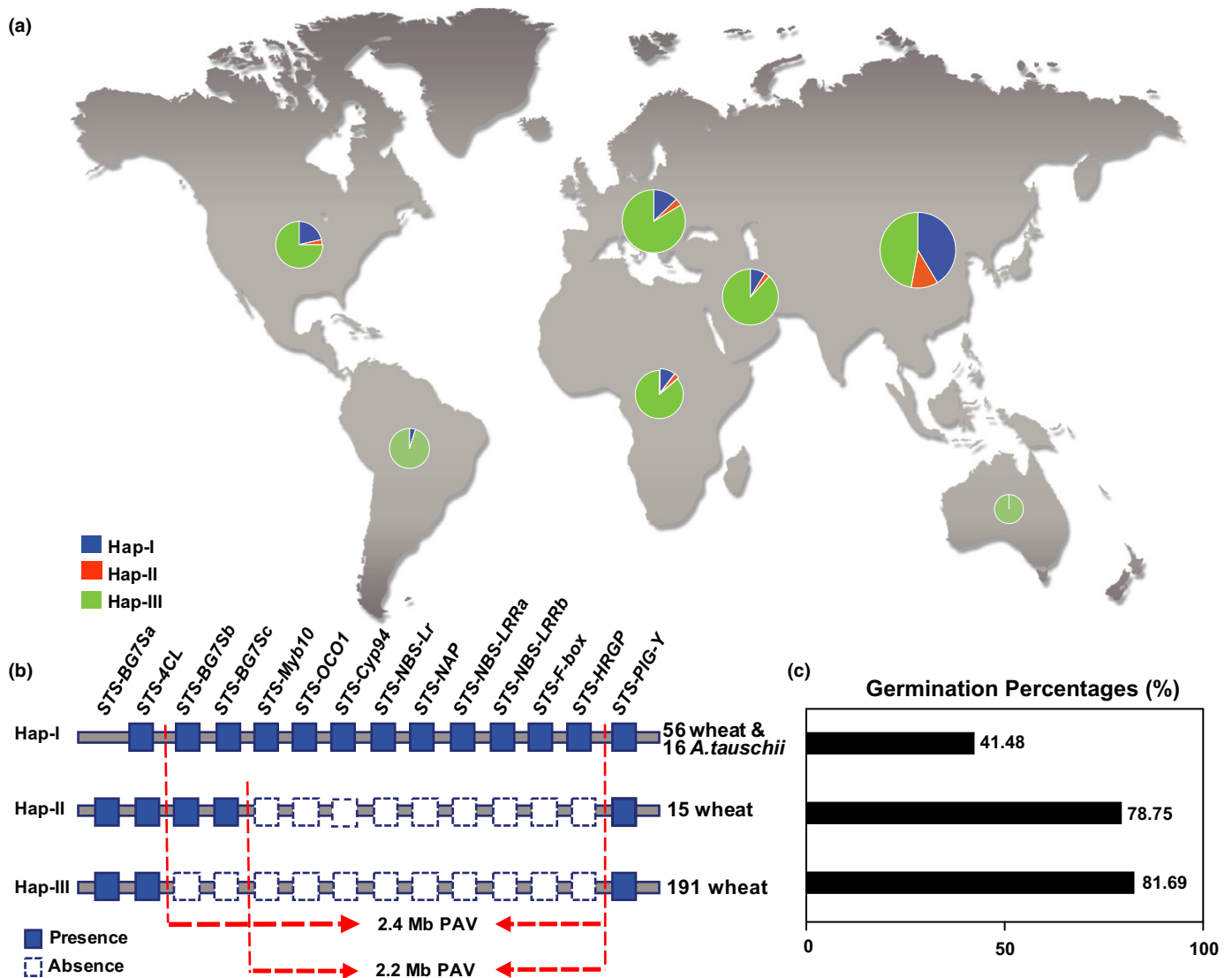
Fig. 2 Presence–absence variation (PAV) of *PHS-3D* in wheat (*Triticeae aestivum*) germplasms. (a) Distribution of three haplotypes (Hap) characterized in 262 wheat and 16 *Aegilops tauschii*. (b) Constitution of the three haplotypes. (c) Average germination percentages of the three haplotypes.

characterization because it has been reported as a QTL controlling PHS resistance (Himi & Noda, 2005).

The PHS-susceptible soft white spring wheat cultivar Fielder (WT) without the 2.4 Mb region (Table S2) was transformed with *Myb10-D* driven by the polyubiquitin promoter (Ubi1). Then, we assessed the *Myb10-D* expression pattern by RNA *in situ* hybridization (Fig. S4). The signals indicated that the expression of *Myb10-D* was concentrated mainly in the mesocarp of the inner pericarp in the positive lines 5–15 DPA. This result was consistent with the observation that *Myb10-D* was predominantly expressed in wheat seeds.

PHS resistance is enhanced in *Myb10-D* overexpressed transgenic wheat

We found that seeds of the OE lines were red-grained, while seeds of the WT control were white-grained (Fig. 3a). Compared to that of the WT, the germination of seeds from the

OE lines was significantly delayed for both whole spike and threshed seeds (Table S7; Fig. 3b). *Myb10-D* led to delayed germination (Fig. 3c) and decreased the GP of 55.1% in threshed seeds and 38.5% in whole spikes (Fig. 3d). The intensity of TTC red coloration in WT seeds was higher than that in seeds from the OE lines and was proportional to seed coat permeability (Fig. 3e). These results support the assumption that the *Myb10-D* identified as *PHS-3D* is involved in PHS resistance in wheat.

Myb10-D regulated the biosynthesis of flavonoids and ABA

Subcellular localization showed that the fused protein 35S:: *Myb10-D:GFP* was located in the nucleus of *Nicotiana benthamiana* leaf protoplasts (Fig. S5). Thus, the nuclear localization of Myb10-D was expected as a transcription factor that is a nuclear protein and may regulate genes during seed development.
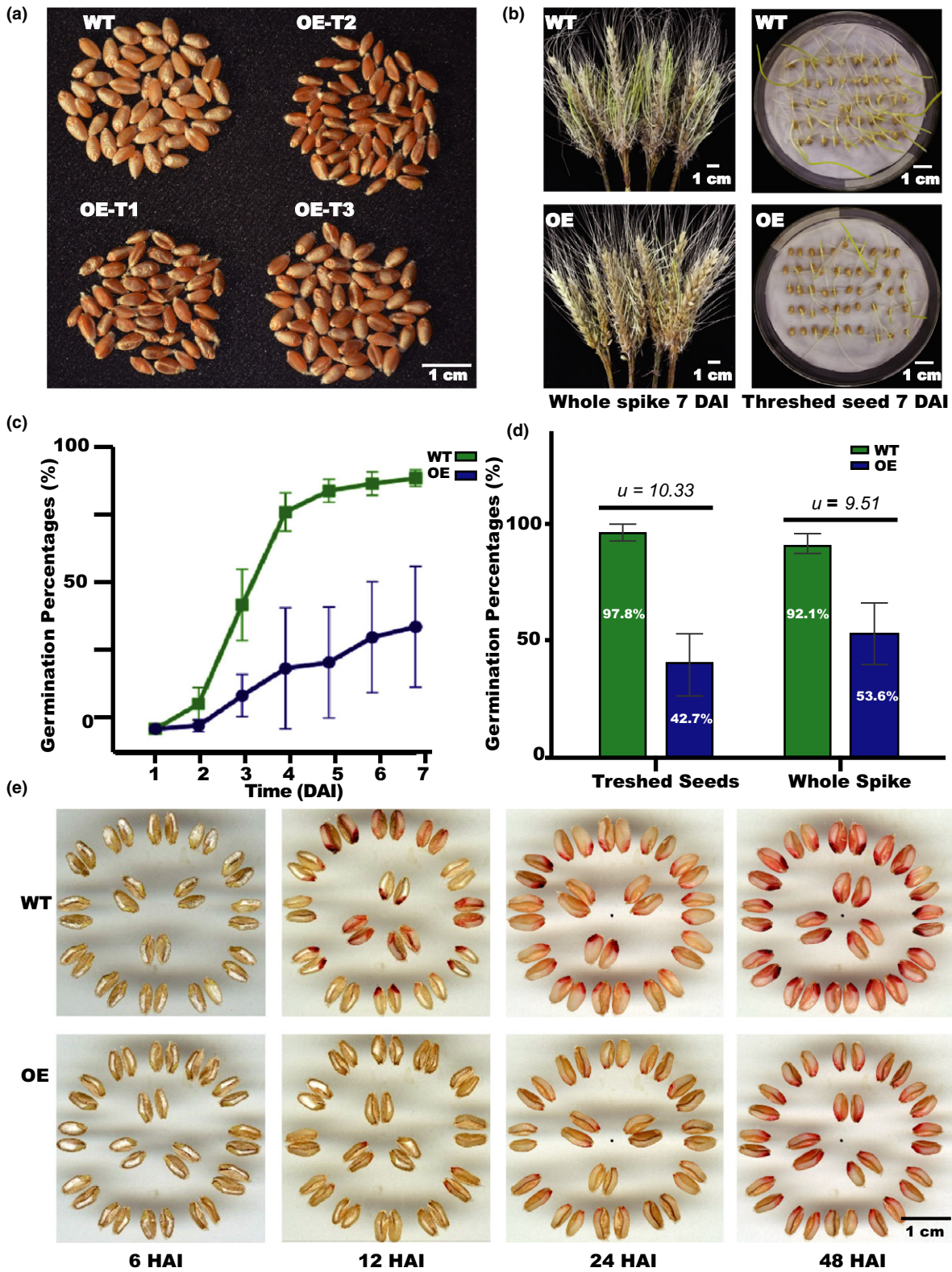
Fig. 3 Characterization of Myb10-D functions in transgenic plants. Phenotypic variation between wild-type (WT) and *Myb10-D* overexpression (OE) wheat (*Triticeae aestivum*) lines, including the germination percentages (GPs) of the whole spikes and thrashed seeds, as well as their seed coat permeability. (a) Profile of seeds in the T1–T3 generations. (b) GP in whole spikes and threshed seeds of OE lines (T3 generation) and WT plants. (c) GP of threshed seeds of OE and WT lines 1–7 d after imbibition (DAI). (d) The GPs were 55.1% and 38.5% lower in the OE lines than in the WT for threshed seeds and whole spike, respectively. (e) Seed coat permeability assumed to be associated with color was assayed by eye. Note: $u > 2.58$ (99% confidence interval); HAI, hours after imbibition. SD, error bars given in the graphs.

The integrated transcriptomic and metabolomic analysis revealed changes in the concentrations of both flavonoids and abscisic acid (ABA) in OE lines compared with WT lines. To uncover the variance in grain color and germination between WT and OE lines, we assayed the expression of genes related to flavonoid and ABA biosynthesis and the accumulation of these compounds by RNA-sequencing (RNA-seq), high-performance liquid chromatography (HPLC), and electrospray ionization triple quadrupole linear ion-trap tandem mass spectrometry (ESI-QTRAP-MS/MS) (Fig. 4). The expression levels (TPM) of *Myb10-D* were 63.19 and 34.21 in the OE lines at 5 DPA and 10 DPA, respectively, while no expression was detected in the WT (Table S8). Genes involved in the methyl-erythritol phosphate (MEP) and flavonoid pathways, which determine the
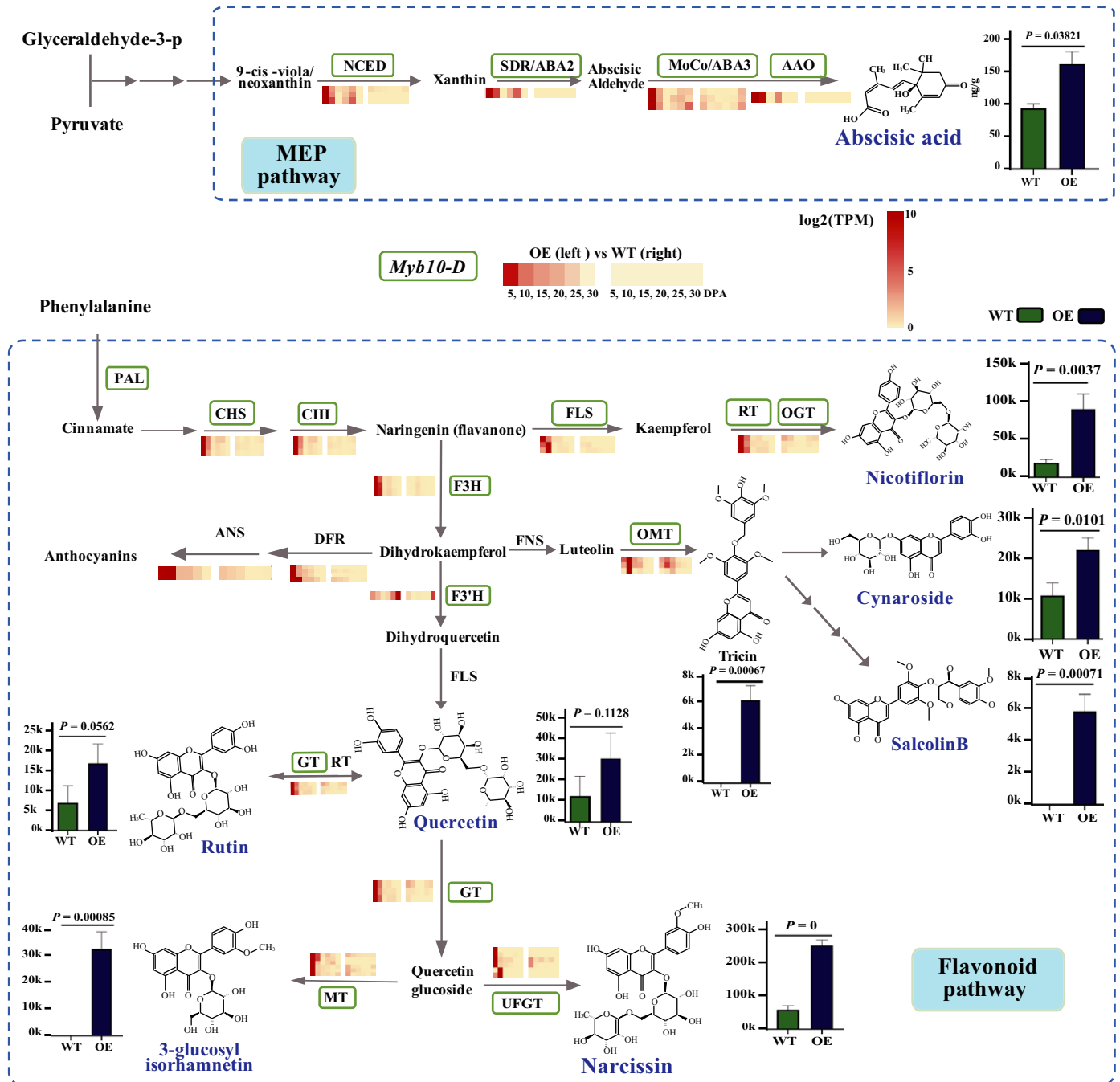

Fig. 4 *Myb10-D* regulates the biosynthesis of flavonoids and abscisic acid (ABA) via the methyl-erythritol phosphate (MEP) and flavonoid pathways in wheat (*Triticeae aestivum*). The details of expression for *ABA2, ABA3, AAO* and *NCED* in the MEP pathway, and *CHS, CHI, F3H, F3'H, ANS, DFR, GT, MT* and *UFGT* in flavonoid pathway are provided in Supporting information Table S8. The accumulations of flavonoid 3-glucosyl isorhamnetin (> 100×), tricin (> 100×), salcolin B (> 100×), nicotiflorin (4.68×), narcissin (4.28×), quercetin (2.45×), rutin (2.41×), cynaroside (2.04×), and ABA (2×) increased (Table S9). SD, error bars given in the graphs.

biosynthesis of flavonoids and ABA (Shirley *et al.*, 1995; Milborrow, 2001), exhibited positive correlations between metabolite and transcript accumulation in the OE lines. *Myb10* was previously described as the *R-1* gene, a seed-specific gene that regulates flavonoid metabolites by promoting the expression of genes (*PAL, FLS, CHS, CHI, F3H, GT, DFR, ANS, F3′H* and *UFGT*) in the biosynthetic pathways (Himi & Noda, 2005; Lai *et al.*, 2013). In this study, eight genes in the flavonoid biosynthesis pathway (*CHS, CHI, F3H, GT, DFR, ANS, F3′H* and *UFGT*) were upregulated in the OE lines (Table S9). Four genes in the MEP biosynthesis pathways (*AAO, NCED, ABA3* and *SDR*) with upregulated expression patterns similar to that of *Myb10-D* were detected. The accumulation of ABA increased one-fold in the seeds from OE compared to WT. And the deeper grain color in the OE lines resulted from the significantly higher biosynthesis of flavonoid 3-glucosyl isorhamnetin, tricin, salcolin B, nicotiflorin, narcissin, quercetin, rutin, and cynaroside (Fig. 3a). The observed increases in both ABA and flavonoids, as well as the upregulation of associated genes, in *Myb10-D* OE lines, indicated that *Myb10-D* also regulates genes in the ABA biosynthetic pathway. The genes associated with flavonoids have been well studied. Thus, we selected *AAO, NCED, ABA3* and *SDR* for a more in-depth examination.

Myb10-D controls germination by positively regulating *NCED* transcription

The expression levels were confirmed by qPCR except for *AAO* whose expression was similar to WT (Figs 5a, S6a). Then 2 kb promoter region of *NCED, ABA3*, and *SDR* was found to carry cis-elements highly similar to the consensus Myb binding secondary wall MYB-responsive element (SMRE) of ACC(A/T)A (A/C)(T/C) and ACC(A/T)ACC(A/C/T) (Grotewold *et al.*, 1994; Zhong & Ye, 2012) (Fig. 5b). To verify possible binding, we carried out an EMSA (Fig. 5c). The Pcold-Myb10-D fusion protein could bind to fluorescently labeled DNA probes containing binding motifs but failed to bind to mutant probes. This binding was not detected under incubated with His protein (without Myb10-D protein). To further examine the specificity of the binding, WT competitors and mutated competitors were introduced. The binding affinities of *ABA3* and *NCED* gradually decreased with increasing concentrations of WT competitor probes but were not affected by mutated competitor probes (Figs 5c, S6b). Adding Myb10-D protein caused reduced gel migration of *ABA3* and *NCED*, indicating the formation of a DNA–protein complex. However, no significant difference was detected for *AAO* or *SDR*.

We used a dual-luciferase reporter (DLR) system to identify how *Myb10-D* affects the expression of *ABA3* (TraesCS7A02G269200) and *NCED* (TraesCS6B02G298800 with 98% identity to *TaNCED*, GenBank: KP0900105). Coexpression of a construct containing the *Myb10-D* full-length coding sequence with the *NCEDpro:LUC* reporter (Fig. 5d) led to significantly higher luciferase (LUC) expression in 35Spro: Myb10-D than in the 35Spro control from both *N. benthamiana* leaves ($P = 0.004$) (Fig. 5e) and *Arabidopsis* protoplasts
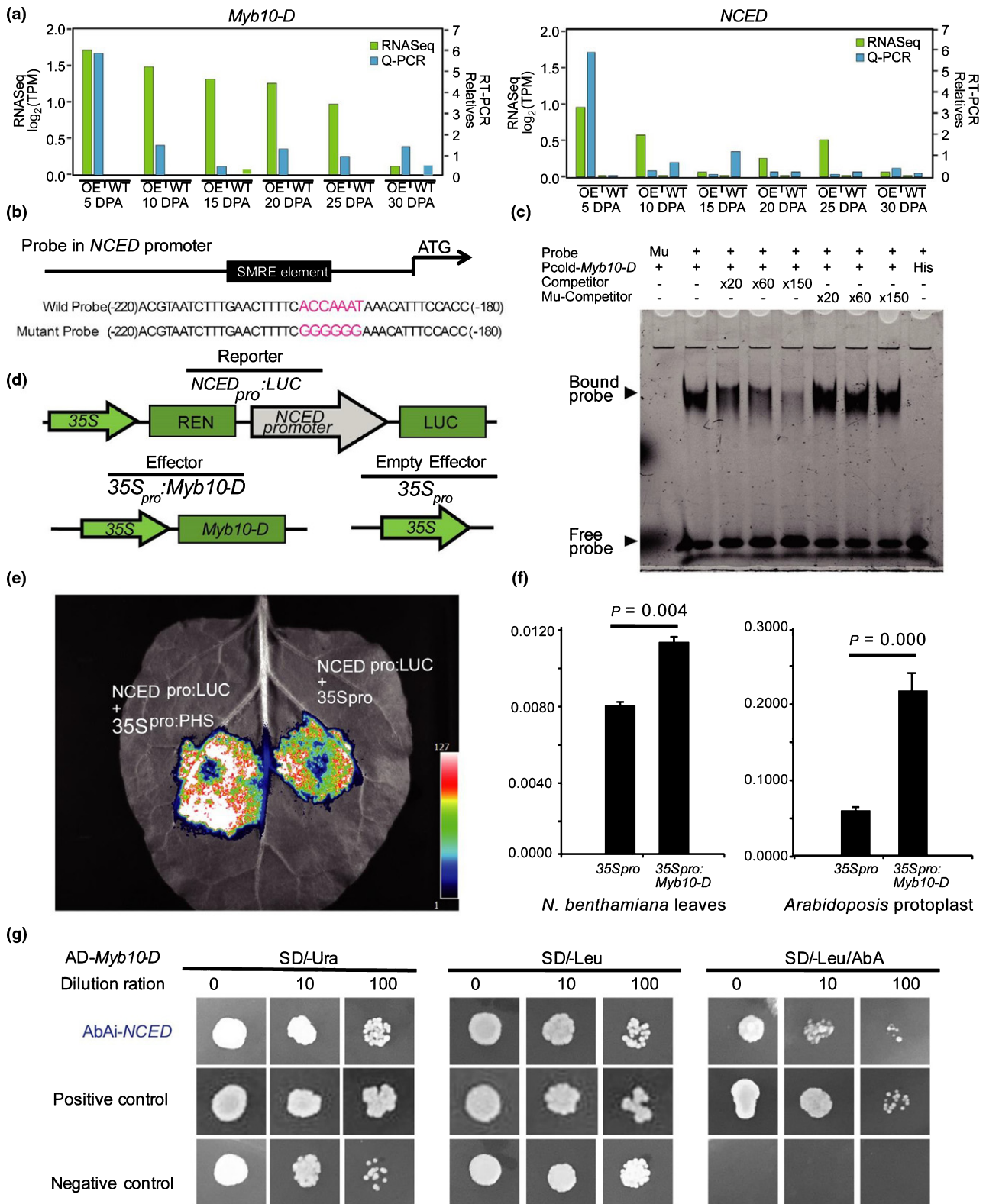
($P = 0.000$) (Fig. 5f), but no significant difference was detected for *ABA3pro:LUC* (Fig. S6c). This result corroborates that *Myb10-D* directly binds to the SMRE at −192 to −199 bp in the *NCED* promoter and functionally activates its expression.

The interaction between *Myb10-D* and the *NCED* promoter was confirmed by a yeast one-hybrid assay (Fig. 5g). The promoter of *NCED* was inserted into the pAbAi vector (Clontech, Japan) and transformed into the Y1H strain. The *NCED* promoter was not activated without protein binding. Yeast containing *Myb10-D* exhibited normal growth under 400 ng ml⁻¹ aureobasidin A (AbA). In contrast, the growth of the negative control cells containing the empty vector was inhibited, which indicated that *Myb10-D* could directly bind to the promoter of *NCED*. Collectively, these results support that *Myb10-D* promotes ABA synthesis, repressing germination by positively regulating *NCED* transcription.

Discussion

We have demonstrated that *Myb10-D* determines PHS resistance by using five complementary approaches: (1) fine mapping of *PHS-3D* that explains up to 42.5% of PHS variation in a 2.4 Mb PAV region; (2) an assessment of the variation of *PHS-3D* and its association with PHS resistance (about 40% lower GP with *PHS-3D* than those without it in globally-sourced wheat germplasms); (3) detection of the mechanism by which *Myb10-D* causes the *PHS-3D* effect by integrated genomic and transcriptomic analyses; (4) phenotyping of plant metabolomic phytohormones, transcriptomes, and germination in transgenic lines (38.5–55.1% lower GP in OE than that in WT lines); and (5) characterization of the role of *Myb10-D* in promoting *NCED* in ABA biosynthesis.

PHS-3D, located in a PAV region, was hard to characterize by regular fine mapping and map-based cloning strategies until recent developments in the omics technology of wheat. Plant genome structural variations, including copy number variations, presence and absence variations, inversions, and translocations, can be beneficial, neutral, or deleterious to the plant (Saxena *et al.*, 2014). In the wheat pangenome project, there were 81070 ± 1631 genes and an average of 128 656 genes in each of 18 elite cultivars compared with CS, and only 2/3 genes shared by all cultivars (Montenegro *et al.*, 2017). Here, we uncover a new case in which the important agronomic traits grain color and PHS among wheat lines are affected by PAV. We found that the dual function *Myb10-D* is in a 2.4 Mb PAV region on 3DL, where unequal crossing over occurred among repetitive LTR TEs with high sequence similarity at the breakpoints (Fig. 1). Because of this large PAV, analyzing the relationship between grain color and germination is difficult without further recombinational events in bi-parental linkage mapping studies. This is the reason that we have known about the relationship between grain color and germination for more than 100 yr, but it has been challenging to uncover the mechanism and to breed white-grained PHS resistant cultivars. Our results indicate the strategy of the white grained PHS resistant wheat cultivar breeding using

(a)

Myb10-D

(b)

Probe in *NCED* promoter

SMRE element ATG

Wild Probe(-220)ACGTAATCTTTGAACTTTTCACCAAATAAACATTTCCACC(-180)
Mutant Probe (-220)ACGTAATCTTTGAACTTTTCGGGGGGAAACATTTCCACC(-180)

(d)

Reporter
NCED_pro:LUC

35S | REN | *NCED promoter* | LUC

Effector
35S_pro:Myb10-D

35S | *Myb10-D*

Empty Effector
35S_pro

35S

(e)

(g)

(c)

NCED

(f)

N. benthamiana leaves

Arabidoposis protoplast

white grained wheat with *Myb10-D*. However, only one white-grained wheat landrace (Tuotuomai/Totoumai) with *Myb10-D* is PHS resistant (Table S2). We will check the variation of the downstream genes associated with the flavonoids pathway in the white dormancy landrace Tuotuomai in the future. This kind of germplasm will be a useful resource for white-grained wheat breeding (Chen *et al.*, 2008; Zhu *et al.*, 2014; Zhou *et al.*, 2017).

Fig. 5 *Myb10-D* binds to the secondary wall MYB-responsive element (SMRE) in the NCED promoter and induces its expression in wheat (*Triticeae aestivum*). (a) The expression profiles of *Myb10-D* (left) and *NCED* (right) 5-30 DPA as detected by RNA-seq and qPCR. (b) Schematic diagram of the 9-cis-epoxycarotenoid dioxygenase (NCED) promoter structure. The SMRE element is −192 to −199 bp away from the ATG of *NCED* (TraesCS6B02G298800). (c) Electrophoretic mobility shift assay (EMSA) of *Mb10-D* with probes containing the binding motifs in the promoters of NCED. The presence (+) or absence (−) of specific probes is indicated. (d) Schematic diagram of various effector and reporter constructs of *NCED*. (e) Dual-luciferase assay of *Myb10-D* in the promoters of NCED in *Nicotiana benthamiana* leaves. (f) Significant differences (Student's *t*-test: *, $P < 0.05$) detected in *N. benthamiana* leaves and *Arabidopsis* protoplasts. Firefly luciferase (LUC) activity was normalized to the Renilla luciferase (REN) activity (as an internal control). Values are means ± SD from three independent replicates for each construct. (g) Yeast one-hybrid analysis of the interaction of *Myb10-D* and the *NCED* promoter. The promoter was used for autoactivation tests in the presence of different concentrations of aureobasidin A (AbA) on SD/-Ura medium, and physical interaction was determined on SD/-Leu medium in the presence of corresponding AbA concentrations.

Myb10-D was significantly ($P < 0.001$) associated with the PHS resistance in wheat varieties and advanced lines (Wang *et al.*, 2016). However, it has been reported that red grain color and seed dormancy can be separated by recombination (DePauw & McCaig, 1983). The ability to separate these traits indicates that grain color and dormancy may be only genetically linked instead of controlled by the same gene (Warner *et al.*, 2000). We observed that in white-grained wheat, in which the 2.4 Mb region on 3DL is absent, the grain is both lighter in color and

germinates faster (Figs 1, 2). White-grained wheat is homozygous for recessive *Myb10-D*, which could lead to both PHS resistance and the red grain phenotype from red-grained wheat. Although the *Myb10-D* in wheat and its D genome donor *A. tauschii* are conserved, it is not present in 22 landraces from Turkey, Iran, India, Nepal, Iraq, Pakistan, and Jordan, indicating that the deletion could have occurred in the early stages of wheat cultivation. Relatives of wild wheat—such as *A. tauschii*—are more dormant (conferring PHS resistance) than domesticated wheat, indicating
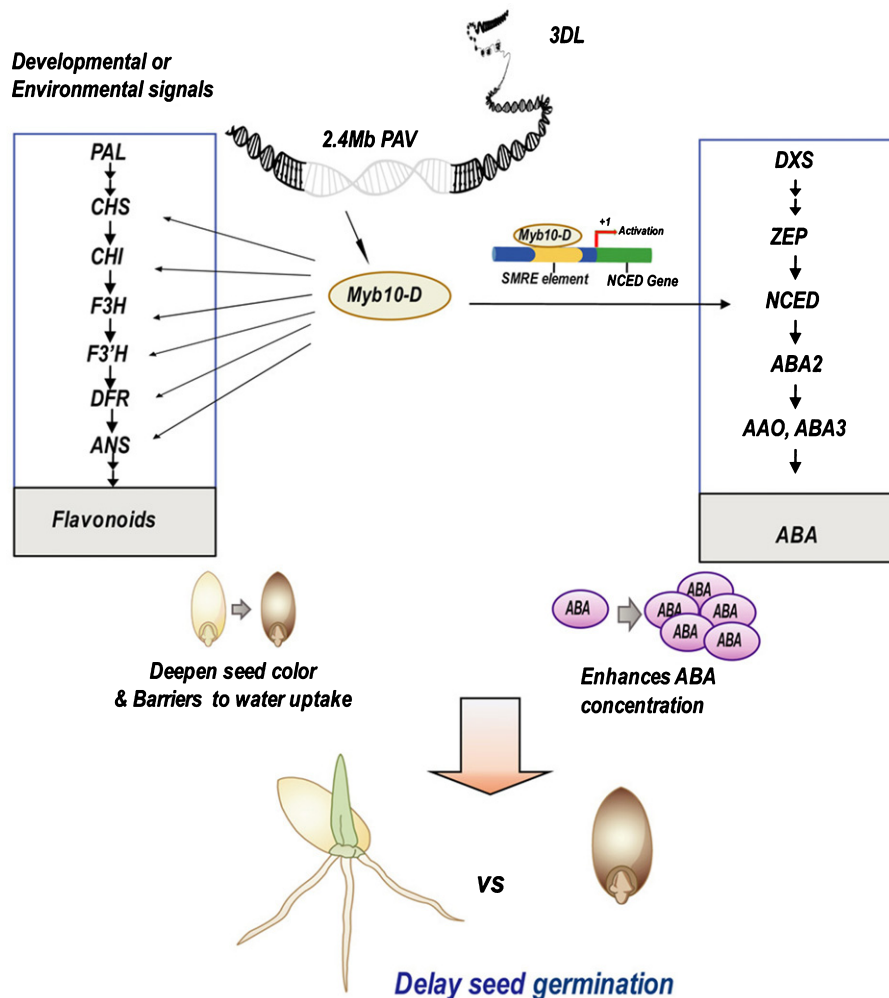

Fig. 6 Hypothetical working model of *Myb10-D* dependent regulation of grain color and germination mediated by flavonoids and abscisic acid (ABA) in wheat (*Triticeae aestivum*). PAV, presence–absence variation; SMRE, secondary wall MYB-responsive element.

that artificial selection has contributed to the reduction of dormancy in modern wheat (Dong *et al.*, 2015; Volis, 2016; Zhang *et al.*, 2017). Likewise, white rice appears to show the domestication syndrome and remains under strong selection in most rice breeding programs (Sweeney *et al.*, 2006). The fact that white-grained wheat is ubiquitous suggests that the deletion also drove the critical transition from the deep seed dormancy and asynchronous germination observed in *A. tauschii* to the shallow and uniform germination observed in wheat cultivars. However, it also resulted in PHS susceptibility.

Our results indicate that *Myb10-D* regulates the transcription levels of genes involved in the MEP and flavonoid pathways, which regulate the biosynthesis of ABA and flavonoids, respectively. Here, the synthesis of ABA and flavonoids was increased, and seed coat permeability was decreased in the *OE* lines (Figs 3, 4). It has been shown that the presence of phenolic flavonoids influences water uptake and may also hinder imbibition, while barriers to water uptake owing to pigmentation may influence dormancy (Huang *et al.*, 1983; Rathien *et al.*, 2009). *NCED* cleaves 9-cis-violaxanthin and 9′-cisneoxanthin to produce xanthoxin as a precursor of ABA and delay wheat seed germination (Kende & Zeevaart, 1997; Tong *et al.*, 2016). In addition to regulating flavonoids, we found that *Myb10* involves the ABA synthesis by promoting *NCED*. Moreover, we will check the ABA levels at more time points during seed development and after-ripening by time-course experiments. We propose a hypothetical working model for the *Myb10-D* dependent regulation of delayed seed germination (Fig. 6). In this model, *Myb10-D* regulates the expression of genes in the flavonoid pathway and regulates *NCED* by binding the SMRE in its promoter region, ultimately affecting the concentrations of flavonoids and ABA. Thus, the dual role *Myb10-D* can regulate both the grain color and seed germination of wheat.

Acknowledgements

Author contributions

Plant materials: MH, DL, YZheng, YWei, PQ, ZP, JM, QJ, GC, LL, LH. Comparative genetics and RNA-seq of candidate genes: MC, JRW, XG, LG, MD, ZC. Divergence of the resistant gene in germplasms: MD, JRW. Experiment design and data analysis: JRW, YWu, M-CL, DL. Fine mapping and map-based clone: JL, JRW, YZhou, LZ, JY, MH, TZ, YY. Gene functional analysis: YF, JL, ML, YL. Manuscript writing: JRW, YZhou, MC, JL, DL, YF, YWu. Phenotype analysis: JL, JRW, ML, ZL, CT. JL, YF and YZhou contributed equally to this work.

ORCID

Ming Hao https://orcid.org/0000-0003-2693-3864
Dengcai Liu https://orcid.org/0000-0001-5508-1125
Ming-Cheng Luo https://orcid.org/0000-0002-9744-5887
Pengfei Qi https://orcid.org/0000-0002-7772-9591
JiRui Wang https://orcid.org/0000-0002-5019-6844
Yongrui Wu https://orcid.org/0000-0003-3822-0511
Lianquan Zhang https://orcid.org/0000-0001-9005-8705

Data availability

The sequence data that support the findings of this study are openly available in NCBI Sequence Read Archive at https://www.ncbi.nlm.nih.gov/, under accession number PRJNA605937. Other main data that supports the findings of this study are available in the Supporting Information of this article.

References

Chen CX, Cai SB, Bai GH. 2008. A major QTL controlling seed dormancy and pre-harvest sprouting resistance on chromosome 4A in a Chinese wheat landrace. *Molecular Breeding* **21**: 351–358.

DePauw RM, McCaig TN. 1983. Recombining dormancy and white seed color in a spring wheat cross. *Canadian Journal of Plant Science* **63**: 581–589.

Dong ZD, Chen J, Li T, Chen F, Cui DQ. 2015. Molecular survey of *Tamyb10-1* genes and their association with grain colour and germinability in Chinese wheat and *Aegilops tauschii*. *Journal of Genetics* **94**: 453–459.

Gordon IL. 1979. Selection against sprouting damage in wheta: III. Dormancy, germinative alpha-amylase, grain redness, and flavanols. *Australian Journal of Agricultural Research* **30**: 387–402.

Groos C, Gay G, Perretant MR, Gervais L, Bernard M, Dedryver F, Charmet G. 2002. Study of the relationship between pre-harvest sprouting and grain color by quantitative trait loci analysis in a white × red grain bread-wheat cross. *Theoretical and Applied Genetics* **104**: 39–47.

Grotewold E, Drunnond BJ, Bowen B, Peterson T. 1994. The myb-homologous P gene controls phlobaphene pigmentation in maize floral organs by directly activating a flavonoid biosynthetic gene subset. *Cell* **76**: 543–553.

Himi E, Maekawa M, Miura H, Noda K. 2011. Development of PCR markers for *Tamyb10* related to R-1, red grain color gene in wheat. *Theoretical and Applied Genetics* **122**: 1561–1576.

Himi E, Nisar A, Noda K. 2005. Colour genes (*R* and *Rc*) for grain and coleoptile upregulate flavonoid biosynthesis genes in wheat. *Genome* **48**: 747–754.

Himi E, Noda K. 2005. Red grain color gene (*R*) of wheat is a Myb type transcription factor. *Euphytica* **143**: 239–242.

Huang G, McCrate AJ, Varriano-Marston E, Paulsen GM. 1983. Caryopsis structural and imbibitional characteristics of some hard red and white wheats. *Cereal Chemistry* **60**: 161–165.

Imtiaz M, Ogbonnaya FC, Oman J, van Ginkel M. 2008. Characterization of quantitative trait loci controlling genetic variation for preharvest sprouting in synthetic backcross-derived wheat lines. *Genetics* **178**: 1725–1736.

The International Wheat Genome Sequencing Consortium (IWGSC), Appels R, Eversole K, Stein N, Feuillet C, Keller B, Rogers J, Pozniak CJ, Choulet F, Distelfeld A et al. 2018. Shifting the limits in wheat research and breeding using a fully annotated reference genome. *Science* **361**: 7191.

Jia J, Xie Y, Cheng J, Kong C, Wang M, Gao L, Zhao F, Guo J, Wang K, Li G et al. 2021. Homology-mediated inter-chromosomal interactions in hexaploid wheat lead to specific subgenome territories following polyploidization and introgression. *Genome Biology* **22**: 26.

Jia M, Guan J, Zhai Z, Geng S, Zhang X, Mao L, Li A. 2018. Wheat functional genomics in the era of next generation sequencing: an update. *Crop Journal* **6**: 7–14.

Jiang L, Zeng X, Wang Z, Ji N, Zhou Y, Liu XT, Chen QM. 2010. Oral cancer overexpressed 1 (ORAOV1) regulates cell cycle and apoptosis in cervical cancer HeLa cells. *Molecular Cancer* 9: 20.

Kende H, Zeevaart J. 1997. The five "classical" plant hormones. *Plant Cell* 9: 1197–1210.

Kihara H. 1944. Discovery of the DD-analyser, one of the ancestors of *Triticum vulgare* (Japanese). *Agriculture & Horticulture (Tokyo)* 19: 13–14.

Lai Y, Li H, Yamagishi MA. 2013. A review of target gene specificity of flavonoid R2R3-MYB transcription factors and a discussion of factors contributing to the target gene selectivity. *Frontiers of Biology* 8: 577–598.

Li J, Yang J, Liu D, Huang R, Sui S, Li M, Zhang Q. 2017. Isolation and characterization of plant *TAF9*, an orthologous gene for TATA-binding protein-associated factor 9, from wintersweet (*Chimonanthus praecox*). *Canadian Journal of Plant Science* 97: 1100–1108.

Liu DC, Lan XJ, Wang ZR, Zheng YL, Zhou YH, Yang JL, Yen C. 1998. Evaluation of *Aegilops tauschii* Cosson for preharvest sprouting tolerance. *Genetic Resources and Crop Evolution* 45: 495–498.

Marroni F, Pinosio S, Morgante M. 2014. Structural variation and genome complexity: is dispensable really dispensable? *Current Opinion in Plant Biology* 18: 31–36.

McFadden ES, Sears ER. 1946. The origin of *Triticum spelta* and its free-threshing hexaploid relatives. *Journal of Heredity* 37: 81–89.

Medina-Puche L, Cumplido-Laso G, Amil-Ruiz F, Hoffmann T, Ring L, Rodriguez-France A, Caballero JL, Schwab W, Munoz-Blanco J, Blanco-Portales R. 2014. *MYB10* plays a major role in the regulation of flavonoid/phenylpropanoid metabolism during ripening of *Fragaria × ananassa* fruits. *Journal of Experimental Botany* 65: 401–417.

Milborrow BV. 2001. The pathway of biosynthesis of abscisic acid in vascular plants: a review of the present state of knowledge of ABA biosynthesis. *Journal of Experimental Botany* 52: 1145–1164.

Miyamoto T, Everson EH. 1958. Biochemical and physiological studies of wheat seed pigmentation. *Agronomy Journal* 50: 733–734.

Montenegro JD, Golicz AA, Bayer PE, Hurgobin B, Lee H, Chan C-KK, Visendi P, Lai K, Doležel J, Batley J et al. 2017. The pangenome of hexaploid bread wheat. *The Plant Journal* 90: 1007–1013.

Morgante M, De Paoli E, Radovic S. 2007. Transposable elements and the plant pan-genomes. *Current Opinion in Plant Biology* 10: 149–155.

Nakamura S. 2018. Grain dormancy genes responsible for preventing pre-harvest sprouting in barley and wheat. *Breed Science* 68: 295–304.

Nilsson-Ehle H. 1914. Zur Kenntnis der mit der keimungsphysiologie des weizens in zusammenhang stehenden inneren faktoren. *Zeitschrift Für Planzenzüctung* 2: 153–187.

Paterson AH, Sorrells ME. 1990. Inheritance of grain dormancy in white-kernelled wheat. *Crop Science* 30: 25–30.

Ransom JK, Bezonsky WA, Sorenson BK. 2006. *Hard white wheat: producing North Dakota's next market opportunity*. North Dakota State University Extension Service, Fargo, ND. [WWW document] URL https://www.ag.ndsu.edu/publications/crops/hard-white-wheat-producing-north-dakotas-next-market-opportunity [accessed January 2015].

Rasul G, Humphreys DG, Brûlé-Babel A. 2009. Mapping QTLs for pre-harvest sprouting traits in the spring wheat cross 'RL4452/AC Domain'. *Euphytica* 168: 363–378.

Rathjen JR, Strounina EV, Mares DJ. 2009. Water movement into dormant and non-dormant wheat (*Triticum aestivum* L.) grains. *Journal of Experimental Botany* 60: 1619–1631.

Roistacher CN, Klotz LJ, Eaks IL. 1957. Ammonia gas used in citrus packing plants as fumigant for control of blue-greenmold on Valencias, navels and lemons. *California Agriculture* 11: 11–12.

Saxena RK, Edwards D, Varshney RK. 2014. Structural variations in plant genomes. *Briefings in Functional Genomics* 13: 296–307.

Schiessl SV, Katche E, Ihien E, Chawla HS. 2018. The role of genomic structural variation in the genetic improvement of polyploid crops. *Crop Journal* 7: 127–140.

Shewry PR, Hey SJ. 2015. The contribution of wheat to human diet and health. *Food Energy Secure* 4: 178–202.

Shirley BW, Kubasek WL, Storz G, Bruggemann E, Koornneef M, Ausubel FM, Goodman HM. 1995. Analysis of *Arabidopsis* mutants deficient in flavonoid biosynthesis. *The Plant Journal* 8: 659–671.

Stetter MG, Vidal-Villarejo M, Schmid KJ. 2020. Parallel seed color adaptation during multiple domestication attempts of an ancient new world grain. *Molecular Biology and Evolution* 37: 1407–1419.

Sweeney MT, Thomson MJ, Pfeil BE, McCouch SR. 2006. Caught red-handed: *Rc* encodes a basic helix-loop-helix protein conditioning red pericarp in rice. *Plant Cell* 18: 283–294.

Tong SM, Xi HX, Ai KJ, Hou HS. 2016. Overexpression of wheat *TaNCED* gene in *Arabidopsis* enhances tolerance to drought stress and delays seed germination. *Biologia Plantarum* 61: 64–72.

Uauy C. 2017. Wheat genomics comes of age. *Current Opinion in Plant Biology* 36: 142–148.

Vetch JM, Stougaard RN, Martin JM, Giroux MJ. 2019. Review: revealing the genetic mechanisms of pre-harvest sprouting in hexaploid wheat (*Triticum aestivum* L.). *Plant Science* 281: 180–185.

Volis S. 2016. Seed heteromorphism in *Triticum dicoccoides*: association between seed positions within a dispersal unit and dormancy. *Oecologia* 181: 401–412.

Walker-Simmons M. 1988. Enhancement of ABA responsiveness in wheat embryos by high temperature. *Plant, Cell & Environment* 11: 769–775.

Walkowiak S, Gao LL, Monat C, Haberer G, Kassa MT, Brinton J, Ramirez-Gonzalez RH, Kolodziej MC, Delorean E, Thambugala D et al. 2020. Multiple wheat genomes reveal global variation in modern breeding. *Nature* 588: 277–283.

Wang JR, Luo M-C, Chen ZX, You FM, Wei YM, Zheng YL, Dvorak J. 2013. *Aegilops tauschii* single nucleotide polymorphisms shed light on the origins of wheat D-genome genetic diversity and pinpoint the geographic origin of hexaploid wheat. *New Phytologist* 198: 925–937.

Wang Y, Wang XL, Meng JY, Zhang YJ, He ZH, Yang Y. 2016. Characterization of *Tamyb10* allelic variants and development of STS marker for pre-harvest sprouting resistance in Chinese bread wheat. *Molecular Breeding* 36: 148–159.

Warner RL, Kudrna DA, Spaeth SC, Jones SS. 2000. Dormancy in white-grain mutations of Chinese Spring wheat (*Triticum aestivum* L.). *Seed Science Research* 10: 51–60.

Yang J, Liu Y, Pu Z, Zhang L, Yuan Z, Chen G, Wei Y, Zheng Y, Liu D, Wang JR. 2014. Molecular characterization of high pI α-amylase and its expression QTL analysis in synthetic wheat RILs. *Molecular Breeding* 34: 1075–1085.

Yang J, Tan C, Lang J, Tang H, Hao M, Tan Z, Yu H, Zhou Y, Liu ZH, Li ML et al. 2019. Identification of *qPHS.sicau-1B* and *qPHS.sicau-3D* from synthetic wheat for pre-harvest sprouting resistance wheat improvement. *Molecular Breeding* 39: 132–143.

Yu M, Chen GY, Zhang LQ, Liu YX, Liu DC, Wang JR, Pu ZE, Zhang L, Lan XJ, Wei YM et al. 2014. QTL mapping for important agronomic traits in synthetic hexaploid wheat derived from *Aegilops tauschii* ssp. *tauschii*. *Journal of Integrative Agriculture* 13: 1835–1844.

Zhang D, He J, Huang L, Zhang C, Zhou Y, Su Y, Li S. 2017. An advanced backcross population through synthetic octaploid wheat as a "bridge": development and QTL detection for seed dormancy. *Fronteir in Plant Science* 8: 2123.

Zhang LC, Dong CH, Chen ZX, Gui LX, Chen C, Li DP, Xie ZC, Zhang Q, Zhang XY, Xia C et al. 2021. WheatGmap: a comprehensive platform for wheat gene mapping and genomic studies. *Molecular Plant* 14: 187–190.

Zhang LQ, Liu DC, Yan ZH, Lan XJ, Zheng YL, Zhou YH. 2004. Rapid changes of microsatellite flanking sequence in the allopolyploidization of new synthesized hexaploid wheat. *Science in China. Series C, Life Sciences* 47: 553–561.

Zhong RQ, Ye ZH. 2012. MYB46 and MYB83 bind to the SMRE sites and directly activate a suite of transcription factors and secondary wall biosynthetic genes. *Plant and Cell Physiology* 53: 368–380.

Zhou Y, Chen ZX, Cheng MP, Chen J, Zhu TT, Wang R, Liu Y, Qi P, Chen G, Jiang Q et al. 2018. Uncovering the dispersion history, adaptive evolution and selection of wheat in China. *Plant Biotechnology Journal* 16: 280–291.

Zhou Y, Tang H, Cheng MP, Dankwa KO, Chen ZX, Li ZY, Gao S, Liu YX, Jiang QT, Lan XJ et al. 2017. Genome-wide association study for pre-harvest

sprouting resistance in a large germplasm collection of Chinese wheat landraces. *Fronteir in Plant Science* 8: 401.

Zhu YL, Wang SX, Zhao LX, Zhang DX, Hu JB, Cao XL, Yang YJ, Chang C, Ma CX, Zhang HP. 2014. Exploring molecular markers of pre-harvest sprouting resistance gene using wheat intact spikes by association analysis. *Crop Journal* 10: 1725–1732.

Supporting Information

Additional Supporting Information may be found online in the Supporting Information section at the end of the article.

Fig. S1 KASP markers were developed by SNPs in the *QPHS.sicau-3D* (*PHS-3D*) region.

Fig. S2 STS markers were developed in the 2.4 Mb PAG region on 3DL for genotyping wheat lines.

Fig. S3 Expression profiles of genes in the PAV region containing *PHS-3D*.

Fig. S4 RNA *in situ* hybridization of *Myb10-D* in transversal sections 5-15 DPA indicates its expression in the mesocarp of the inner pericarp.

Fig. S5 Subcellular localization of Myb10-D in the nucleus.

Fig. S6 Characterization of binding sites based on the 2-kb promoter regions of potential *Myb10-D* regulated genes in the MEP pathway.

Methods S1 DNA extraction and genotyping.

Methods S2 Fine mapping of *PHS-3D* (*QPHS.sicau-3D*).

Methods S3 Optical map construction.

Methods S4 Gene cloning and sequencing.

Methods S5 RNA preparation and RNA sequencing.

Methods S6 NGS data analysis (reads mapping, assembly, and functional annotation).

Methods S7 Quantitative PCR with reverse transcription (RT)-PCR.

Methods S8 Gene transformation.

Methods S9 Endogenous ABA profiling.

Methods S10 Flavonoids extraction and profiling (multiple reaction monitoring, MRM).

Methods S11 Subcellular localization of *Myb10-D*.

Methods S12 RNA *in situ* hybridization.

Methods S13 Protein expression in *Escherichia coli* and purification.

Methods S14 Electrophoretic mobility shift assay.

Methods S15 Transient expression assay.

Methods S16 One-hybrid assays in yeast.

Methods S17 Statistical analyses.

Methods S18 Code used in this study.

Table S1 Primers used for KASP, STS, PCR clone, qPCR, transgenetic, and transactivation assay.

Table S2 Genotyping and phenotyping of 262 common wheat, 16 *Aegilops tauschii*, and three tetraploid wheat lines.

Table S3 Summary of genomic reference sequences data and NGS data obtained in this study (NCBI, PRJNA605937).

Table S4 Genes in the 2.4 Mb PAV region from six accessions CS, AK58, AL8/78, Robigus, Cadenza, and SHW-L1.

Table S5 Transposons in the 2.4 Mb PAV region from CS and AK58.

Table S6 The expression of 20 genes in 2.4 Mb PAV region from CM32 and SHW-L1 in 10-30 DPA seeds, and the expression of three selected genes from CS and BCScv1 in 29 tissues or stages.

Table S7 Germination percentages of WT and OE lines.

Table S8 Different expression genes that had similar expression patterns with Myb10-D form WT and OE lines in 5-30 DPA seeds.

Table S9 Accumulation of flavonoids and ABA in WT and OE lines.

Please note: Wiley Blackwell are not responsible for the content or functionality of any Supporting Information supplied by the authors. Any queries (other than missing material) should be directed to the *New Phytologist* Central Office.